*Romanian Reports in Physics, Vol. 68, No. 3, P. 1085–1096, 2016*

# FILTRATION OF FLUE GAS BY RETAINING OF NANOPARTICLES IN MICROFLUIDIC DEVICES USING DIELECTROPHORESIS

ADRIAN NECULAE, MADALIN BUNOIU, ANTOANETTA LUNGU, MIHAI LUNGU*

West University of Timisoara, Faculty of Physics, 4 V. Parvan, 300223 Timisoara, Romania
*Corresponding author: lmihai@physics.uvt.ro

*Received January 25, 2015*

*Abstract.* The burning processes are responsible for the emission in the environment of a significant amount of nanoparticles. As the presence in the environment of nanoparticles with size ranging from 50 nm to 150 nm has been shown to have a profound impact on human health, the filtration of nanoparticles suspended in flue gas became an important technological challenge. In this context, the nanoparticle manipulation using strongly non-uniform electric fields, and especially dielectrophoresis (DEP), proved to be an extremely efficient tool.
This paper presents an experimental DEP-based micro-system used for the selective retaining of nanoparticles suspended in a gaseous environment. The particles deposited on the electrodes are analyzed using a reflection metallographic microscope with CCD camera and a data analysis system. The experimental results highlight the deposition of nanoparticles on electrodes and the fact that the concentration of captured particles diminishes as one depart from the input region, in concordance with our simulation results.

*Key words*: flue gas, recovery, dielectrophoresis, nanoparticles, numerical simulation.

## 1. INTRODUCTION

In recent years, many new methods of construction have been proposed with the goal of increasing flue gas filtration efficiency, particularly for nanoscale particles [1, 2]. The presence in the environment of nanoparticles with size ranging from 50 nm to 150 nm was proved to have a profound impact on human health. This category of particles is massively generated during industrial emissions (material synthesis, combustion processes, etc) and is highly toxic due to their large specific surface area. Once inhaled, they may generate free radicals, affect the DNA, and alter the genes, which lead to increased cancer risk and incidence of mutagen and teratogenic-related phenomena, carcinogenic effects or causing a variety of lung-disease typologies [3–6]. The sources of polluting emissions are

generally equipped with different filters that capture only micron particles, while all the nanoparticles escape in the air. All the traditional methods attempted for manipulating (retaining and separating) nanoparticles from gas suspensions have not been efficient (because only a small part of the particles is collected and only when they attach to larger particles) [3, 7].

The methods utilizing *dielectrophoresis* (DEP) proved to be the most promising techniques for nanoparticle trapping and controlled spatial separation [7–9]. The phenomenon of DEP originates from the interaction of the induced dipole moment with the applied electric field. The DEP force does not require electrically charged particles; the strength of the force depends on the medium and particle's electrical properties, particle's shape and size, and on the applied electric field amplitude and frequency [10, 11]. Microelectrodes integrated into microfluidic devices can generate large electric fields and field gradients using low voltages. The field gradients can be used to actively drive the motion of suspended nanoparticles in a flue gas by dielectrophoresis [3, 8, 9, 12].

In this paper, we use mathematical modeling, computer simulations and do experiments to investigate the filtration of flue gas by trapping of suspended nanoparticles in a microfluidic device using positive dielectrophoresis. The numerical simulations presents a set of results describing the behavior of nanoparticles with sizes ranging from 50 to 150 nm in a DEP-based microsystem, which consists in a microchannel-working unit of a particulate trap. The concentration of nanoparticle suspension inside the microfluidic separation device is analyzed in terms of a new specific quantity of separation process, called *Filtration rate*. In the second part, the performance of an experimental microfluidic device for retaining of nanoparticles from flue gas is analyzed in terms of another new specific quantity of separation process, called *Recovery*, which highlights the capability of the device to capture the nanoparticles. The numerical analysis combined with the experimental investigations lead to the improvement of the mathematical model and optimization of the experimental device, in order to be useful in designing of microfluidic devices for separating nanoparticles from flue gas.

## 2. THEORETICAL CONSIDERATIONS

The time averaged dielectrophoretic (DEP) force acting on a spherical particle situated in an AC electric field can be written as [5, 7, 10]:

$$\left\langle \mathbf{F}_{DEP} \right\rangle = 2\pi a^3 \varepsilon_m \operatorname{Re}\left[ \tilde{K}(\omega) \right] \nabla \left( \left| \nabla V_R \right|^2 + \left| \nabla V_I \right|^2 \right), \tag{1}$$

where $a$ is the particle radius, $\omega$ the angular field frequency and $\mathrm{Re}[\tilde{z}]$ indicates the real part of a complex phasor $\tilde{z}$. $V_R$ and $V_I$ are the real and imaginary parts of the electric potential phasor, $\tilde{V} = V_R + \mathrm{j}V_I$. For a homogeneous medium, the electric potential phasor satisfy the Laplace equation $\nabla^2\tilde{V} = 0$. The quantity $\tilde{K}(\omega) = \left(\tilde{\varepsilon}_p - \tilde{\varepsilon}_m\right)/\left(\tilde{\varepsilon}_p + 2\tilde{\varepsilon}_m\right)$, named the complex Clausius–Mossotti (CM) factor, is a measure of the effective polarizability of the particle, where $\tilde{\varepsilon}_p$ and $\tilde{\varepsilon}_m$ are the complex dielectric permittivities of particles and medium, respectively. The complex permittivity is defined as $\tilde{\varepsilon} = \varepsilon - \mathrm{j}(\sigma/\omega)$, where $\sigma$ is the electrical conductivity and $\mathrm{j} = \sqrt{-1}$. The CM factor depends on the dielectric properties of the particles and medium and on the frequency of the applied electric field; at low frequencies, its sign is determined by the electrical conductivities of the particle and the medium, and at higher frequencies by the corresponding permittivities [5, 9, 10]. The variation in the real part of this factor results in a frequency-dependent dielectrophoretic force that is specific for a particular type of particle. Therefore, DEP force represents an effective tool for separating particles, based solely on their dielectric properties and size. When the sign of $\mathrm{Re}\left[\tilde{K}(\omega)\right]$ is positive, the particles are attracted to the locations of electric field intensity maxima and repelled from the minima, phenomenon known as positive dielectrophoresis (pDEP). The opposite occurs when $\mathrm{Re}\left[\tilde{K}(\omega)\right]$ is negative, situation referred to as negative dielectrophoresis (nDEP).

The macroscopic behavior of a suspension of spherical particles of radius $a$ in a fluid of viscosity $\eta$ is modeled by considering the mechanical equilibrium between an external force **F** (DEP force in this case) and the Stokes drag force. In this context, the dynamics of a system of small particles (*i.e.* nanoparticles) suspended in a compressible fluid is governed by the following system of equations [10]:

$$\mathbf{v} = \mathbf{u} + \frac{2a^2}{9\eta}\mathbf{F}\ , \tag{2a}$$

$$\frac{\partial C}{\partial t} + \nabla\cdot\mathbf{j} = 0\ ,\ \text{where}\ \ \mathbf{j} = C\mathbf{v} - D\nabla C\ . \tag{2b}$$

Here **u** and **v** are the fluid and particle velocities, $t$ is the time, **j** – the particle flux, $D$ is the diffusion coefficient of the particles, and $C$ is the particle volumic concentration.

A typical DEP-based separation device with parallel interdigitated bar electrodes placed on the bottom surface is illustrated in Fig. 1.

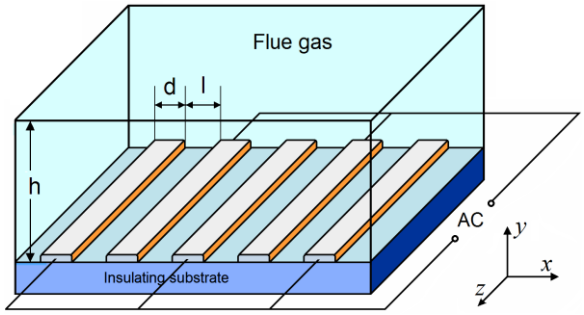


Fig. 1 – Schematic representation of experimental device used for DEP separation.

In most of the reported mathematical models, due to the symmetry of the geometry and considering the electrodes much longer than their width, the problem is treated in two dimensions and the electrodes' height is neglected. By taking into account the periodic distribution of the electrodes, the numerical calculations of the DEP force and the concentration field can be performed considering as computational domain only a so called "basic unit cell", which fully describes the entire system, except the vicinity of the device walls. The geometry of the computational domain, together with the associated boundary conditions necessary to solve the Laplace equation for electric potential $V_R$ are presented in Fig. 2. Similar boundary conditions hold for the imaginary part of the electric potential, $V_I$ [9].

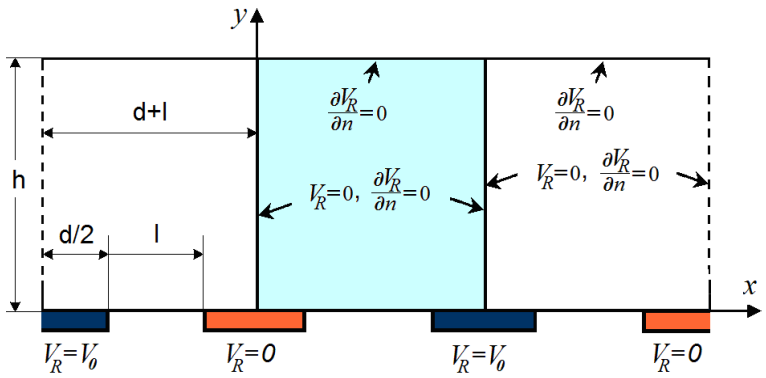


Fig. 2 – The geometry of the computational domain and the associated boundary conditions for the electric potential $V_R$. The basic unit cell is indicated by solid lines.

The fluid flow field inside the separation device, **u**, is calculated by solving the classical Navier-Stokes equation in the compressible case, together with the corresponding boundary conditions [9]. For the obtained DEP-force and fluid flow field, the concentration of suspended particles is evaluated by numerically integrating equations (2a) and (2b). The calculated concentration field gives information at a local scale, showing how the particles are attracted to the margins of electrodes and the influence of the main parameters of the problem on this process.

If one notes $C_0$ and $C$ the mean concentrations of suspended nanoparticles at the input of the device, and after a certain number of cells (electrodes), as schematically sketched in Fig. 3, the global effect of the dielectrophoretic forces on suspended particles can be evaluated by computing the average concentration of particles for every unit cell inside the microfluidic device. The analysis of the variation of this quantity along the device is an appropriate tool in order to evaluate the efficiency of the filtration process.

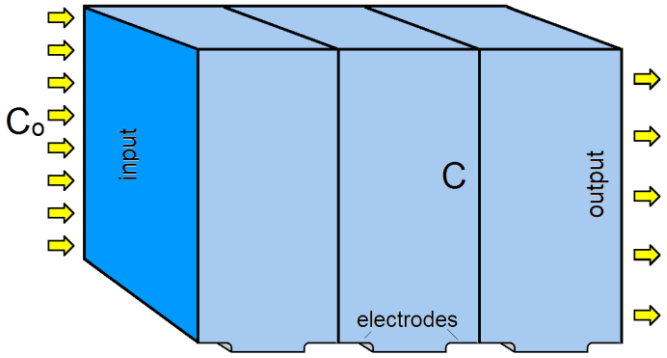


Fig. 3 – Schematic representation of the separation device revealing the concentrations of the suspended nanoparticles at the input and the output surfaces of the device.

### 3. NUMERICAL RESULTS

In this section we present a set of results obtained by numerical simulation of the behavior of a nanoparticle suspension in gas, inside a typical dielectrophoretic separation device, in terms of the mathematical model previously described. We analyze and discuss the obtained numerical results in terms of *Filtration rate*, a global quantity correlated with the concentration field, which offers a more suggestive characterization of the capabilities of the device regarding the separation process of nanoparticles from flue gas. All the numerical simulations were performed using the *COMSOL Multiphysics* program.

For the computation of the pDEP force, we first solved the Laplace equation for the real and imaginary components of the electric potential, together with the associated boundary conditions presented in Fig. 2. The computational domain consists of a unit cell described by the following set of geometric parameters: $d = l = 100$ μm and $h = 500$ μm. The simulations were performed for a suspension of particles with characteristic sizes $a$ = 50 nm, $a$ = 100 nm and $a$ = 200 nm respectively, in air. The dielectric response of the particles is characterized by the real part of the CM factor $K_R = 1$ and we considered the amplitude of the electric potential applied on the electrodes varying in the range $V_0 = 12 \div 24$ V.

The efficiency of the filtration process is evaluated by calculating the variation of the particles concentration along the dielectrophoretic device for different values of problem's parameters. The computation is performed using an iterative procedure: the output concentration in one unit cell is considered to be the input concentration for the next unit cell, in order to describe the cumulative effect of the filtration inside the microfluidic device. This type of analysis allows an estimation of the necessary number of cells (or electrodes) in order to obtain a certain output level for the concentration of suspended particles, when the other parameters of the problem are fixed. The results presented in Figure 4a show that, for example, in the case of particles having size of 100 nm, a desired diminishing concentration rate of 90% can be obtained by using about 30 electrodes when applying a voltage of 24 V, about 60 electrodes for 18 V, and about 200 electrodes for an applied voltage of 12 V.

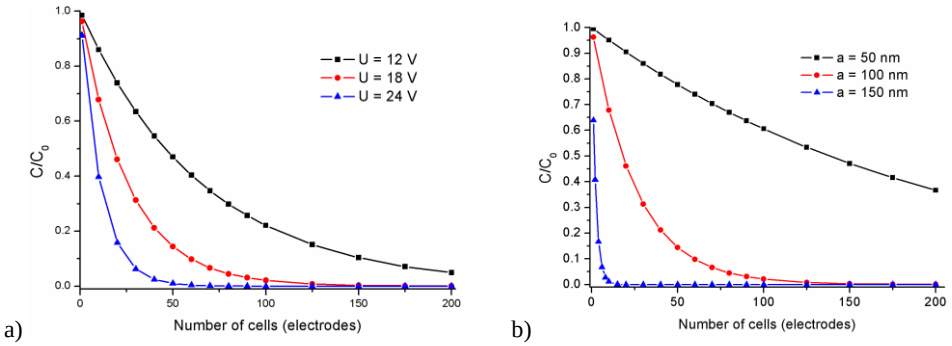


Fig. 4 – Calculated mean particles concentration *versus* number of cells for: a) particles with $a$ = 100 nm at three different applied voltages and b) particles with three different radii at a fixed applied voltage of $V_0 = 18$ V ($d = l$ = 100 μm).

When we analyze the effect of particle radii on the filtration efficiency, the results presented in Fig. 4b predict that, for example, when the applied voltage is 18 V, particles of 150 nm are completely captured after 10 cells, for particles of

100 nm we need about 150 electrodes for the complete capture, while the particles of 50 nm are captured less than 60% even if one use devices with 250 electrodes.

In conclusion, the simulations performed in the frame of the presented mathematical model allow an estimation of the performances of the dielectrophoretic filtration process as a function of the geometric and physical parameters of the problem.

## 4. EXPERIMENTAL RESULTS

Based on the results obtained from the mathematical model and numerical simulations, it was realized and tested a laboratory microfluidic device for retaining nanometric particles in non-uniform electric field by positive dielectrophoresis (pDEP). Practical tests were conducted on an emission source represented by a pilot plant for incineration of different waste categories. The main active parts of the device consist of the deposition plates, made by PCB (Printed Circuit Board) technique (Fig. 5), with electrode width and gap between electrodes $d = l = 100$ μm.

a)  b) 

Fig. 5 – a) Deposition plate made by PCB technique; b) detail of interdigitated electrodes.

We performed experiments for nanoparticle trapping from flue gas by injecting smoke at the bottom of the experimental device. The outline of the laboratory experimental device is presented in Fig. 6a, and a detail with experimental device under work conditions (with flue gas fumigation at the bottom), is shown in Fig. 6b.

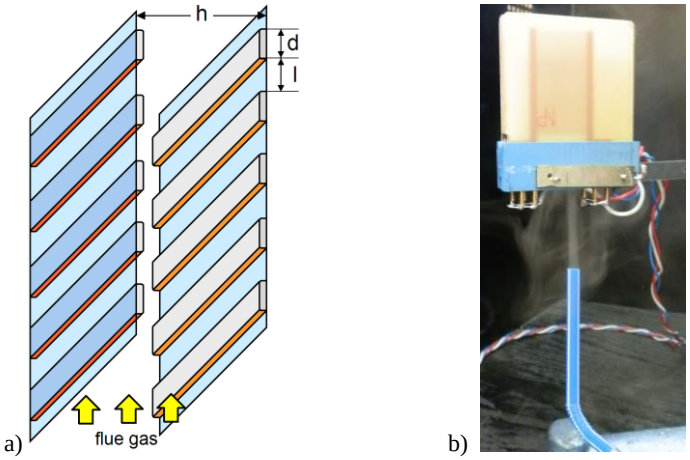


Fig. 6 – a) The outline of the laboratory experimental device,
and b) device at work with flue gas at the bottom.

Figure 7 presents the equipment used for the analysis of the deposition plates, consisting in a reflection metallographic microscope with CCD camera and the related computer, during the investigation of a deposition plate before fumigation, in the absence of the applied voltage. On the screen it appears a snapshot with a detail of the deposition plate obtained at a 100 × magnitude. The vertical light stripes on the display are the electrodes, while the dark stripes are the gaps.

Fig. 7 – The equipment for the analysis of the deposition plates;
on screen appears a snapshot of a detail of the deposition plate obtained at 100 ×.

The tests performed with a DEP-based separation device having $l = d = 100$ μm and $h = 2$ mm reveal that in the absence of the applied voltage the particles are not at all attracted to the electrodes, while once applied an AC voltage, the dielectrophoretic effect appears. In the absence of the applied voltage, the nanoparticles suspended in the flue gases are not attracted on the electrodes and, therefore, will not deposit on the plates. By applying an AC voltage, the deposition phenomenon occurs due to positive dielectrophoresis.

Figure 8 shows successive video frames (snapshots) representing the deposition of nanoparticles from the injected smoke on the collection plates by pDEP. On the electrodes were applied AC signals of various amplitudes and forms (sinusoidal and rectangular). Snapshots were performed at different distances from the top of the experimental device, where one obtain a minimum density of the collected material *versus* the bottom, where the density of deposited nanoparticle is the greatest. The figure shows a decreasing in the concentration of captured nanoparticles, from the entrance toward the exit area. As the smoke "climbs" inside the device, particles in suspension are lost by their accession to the collection plate, the result being in accordance with the theoretical considerations and the numerical simulations.

For a quantitative analysis of the filtration process, we define the parameter *Recovery* (*R*), representing the performance or effectiveness of the separation, related to the particles that are deposed on the electrodes after the fumigation, by analyzing the images from Fig. 8. The analysis was performed using the Image Analyzer software, which offers information regarding the "black degree" of each snapshot from Fig. 8, as a function of the density of particles located on the deposition plates of the microfluidic device after fumigation:

$$R = \frac{C_i}{C_{\max}}, \tag{4}$$

where $C_i$ is the calculated value of the particle density on a snapshot $i$ (corresponding to a certain number of cells on the vertical direction) and $C_{\max}$ is the calculated value of the maximum particle density at the input of the experimental device (at the bottom in Fig. 8).

The results presented in Fig. 9 reveal two important things: on the one hand, the Recovery is improved when one use higher amplitudes of the applied signal, and, one the other hand, for the same amplitude of the applied signal, the recovery rate is better when one use sinusoidal signals, compared to rectangular signals.

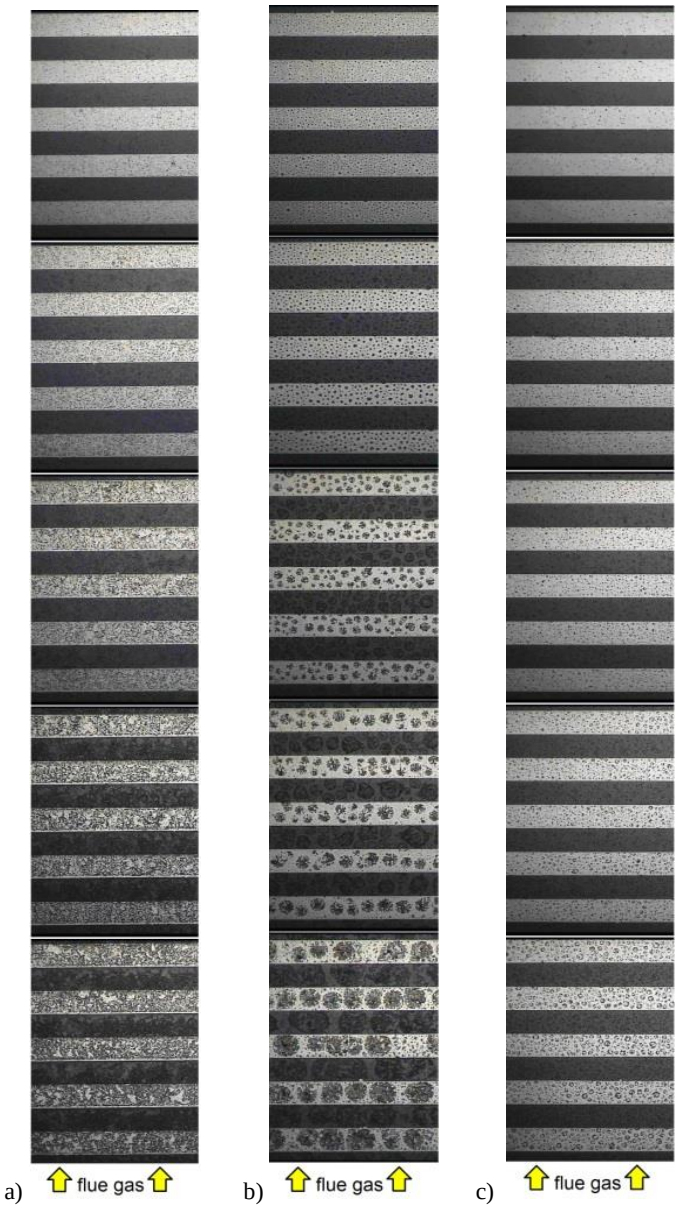


Fig. 8 – Successive snapshots revealing the results obtained after fumigation with the DEP-based separation device with $l = d = 100$ μm, $h = 2$ mm, at: a) $U = 24$ V, AC sinusoidal signal, $f = 50$ Hz, time of fumigation $t = 30$ s; b) $U = 12$ V, AC sinusoidal signal, $f = 50$ Hz, time of fumigation $t = 30$ s; c) $U = 12$ V, AC rectangular signal, $f = 100$ Hz, time of fumigation $t = 30$ s. A decreasing in the concentration of captured nanoparticles, vertically from the entrance towards the exit area is observed in all cases.

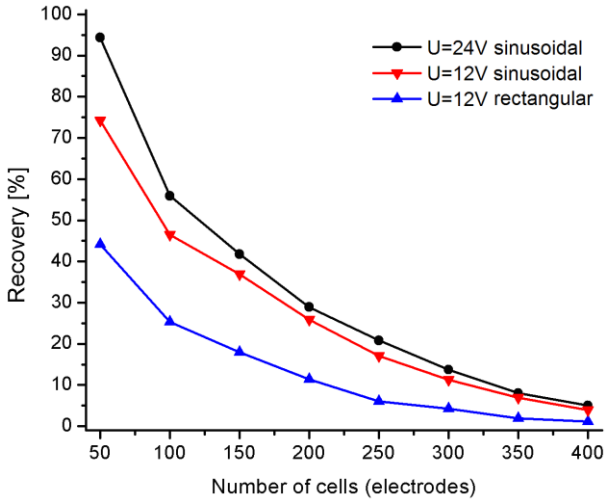


Fig. 9 – Recovery, *versus* the number of cells, determined for the DEP-based separation device with $l = d = 100$ µm, $h = 2$ mm, at: i) $U = 24$ V, AC sinusoidal signal, $f = 50$ Hz, time of fumigation $t = 30$ s; ii) $U = 12$ V, AC sinusoidal signal, $f = 50$ Hz, time of fumigation $t = 30$ s, and iii) $U = 12$ V, AC rectangular signal, $f = 100$ Hz, time of fumigation $t = 30$ s, by analyzing the images from Fig. 8. A decreasing of captured nanoparticles on the electrodes with the distance is observed.

## 5. CONCLUSIONS

This contribution presents both an theoretical and an experimental study of a DEP-based microsystem for the selective manipulation of nanoparticles using dielectrophoresis. Based on a mathematical model and numerical simulations, we build-up an experimental device for retaining the nanoparticles from combustion gases in non-uniform electric field, and then we used it for performing experiments on nanoparticle trapping from smoke.

The numerical study focuses on evaluation of the effectiveness of filtering nanoparticle from combustion gases in a microfluidic device using positive dielectrophoresis. This type of analysis allow the estimation of the number of cells (or electrodes) required to achieve a desired output level for the concentration of suspended particles, for different particles radii or different applied voltages on the electrodes, when the other parameters of the proposed model are fixed.

Based on the results obtained from mathematical modeling and numerical simulations, it was designed, developed and tested a laboratory microfluidic device for retaining of nanometric particles from smoke by positive dielectrophoresis. The experiments performed with this device, at applied voltages of different amplitudes and forms (sinusoidal and rectangular), highlight, in all investigated cases, the deposition of nanoparticles on electrodes and the fact that the concentration of

captured particles decreases as we move away from the entrance area of the smoke resulted from the combustion of different wastes, the results being in good agreement with the numerical simulations. The recovery rate increases with the amplitude of the applied signal and is higher for sinusoidal signals, compared to rectangular signals.

This state of the art of the presented mathematical model and microfluidic system design is still subject of future improvements and represents both a significant challenge and opportunity for the microfluidic research community.

***Acknowledgments.*** This work was supported by a grant of the Romanian National Authority for Scientific Research, CNCS – UEFISCDI, project number PN-II-ID-PCE-2011-3-0762.

REFERENCES

1. D. Rickerby, M. Morrison, JRC Ispra. (2007); www.nanowerk.com/nanotechnology/reports/reportpdf/report101.pdf.
2. C. Barbaros, L. Dongqing, Electrophoresis **32**, 2410–2427 (2011).
3. M. Chang, C. Huang, J. of Environ. Eng. **127**, 78–81 (2001).
4. A. Gatti, S. Montenari, *Nanoparticles' Promises and Risks*, Springer, Heidelberg, New York, Dordrecht, London, 2014, pp. 71–87.
5. P. Minutolo, L. Sgro, M. Costagliola, M. Prati, M. Sirignano, A. D'Anna, Chem. Eng. Trans. **22**, 239–244 (2010).
6. S. Shegokar, *Nanoparticles' Promises and Risks*, Springer, Heidelberg, New York, Dordrecht, London, 2014, pp. 87–103.
7. H. Morgan and N.G. Green, *AC Electrokinetics: Colloids and nanoparticles*, Research Studies ltd. Baldock, Hertfordshire, 2003.
8. N. G. Green, A. Ramos, H. Morgan, J. Elstat. **56**, 235–254 (2002).
9. M. Lungu, A. Neculae, M. Bunoiu, J. of Optoelectronics and Advanced Materials **12**, 2423–2426 (2010).
10. A. Neculae, C. Biris, M. Bunoiu, M. Lungu, J. Nano. Res. **14**, 1–12 (2012).
11. R. Pethig, Biomicrofluidics **4**, 022811–1 – 02281–34 (2010).
12. F. Sbrizzaia, P. Faraldib, A. Soldatia, Chem. Eng. Sci. **60,** 6551–6563 (2005).